Time-resolved Fourier spectroscopy for activated optical materials

H. Weidner and R. E. Peale

A low-cost add-on to commercial Fourier-transform spectrometers that have a continuously scanning Michelson interferometer has been developed for high-resolution, broadband, time-resolved spectroscopy. A number of innovations have been implemented to enable near-IR, visible, and UV photoluminescence studies. These include error correction and normalization of interferogram points to correct for laser intensity variations and missed shots, reduction of mirror-speed variations with recognition and avoidance of the timing mistakes they cause, and simple white-light-interferogram advancement optics that leave high-frequency modulation efficiency for the signal of interest unchanged in dynamically aligned systems. Application to energy-transfer phenomena in solid-state-laser media is described.

Key words: Time resolved, Fourier, spectroscopy, laser crystals.

1. Introduction

Time-resolved Fourier-transform spectroscopy (TRFTS) is a developing technique with great promise. There are two main approaches, which differ in their method for mirror advancement in the moving arm of the interferometer: step scan and continuous scan. For step scan, the mirror is fixed at a precisely known position while transient events are sampled and then stepped to a new position. After the desired maximum optical path-length difference has been reached, the data are sorted into a series of interferograms, each corresponding to a different time delay. Step scan has the advantage of decoupling the spectral multiplexing from the time dependence of the phenomenon studied. Disadvantages are the difficulty in precisely maintaining a fixed mirror position during signal averaging and the required stabilization and position-sensing hardware, which are especially complex for visible and UV measurements.

The continuous-scan method can be divided into three approaches of varying difficulty. The easiest is rapid scan, in which the time dependence of the phenomenon of interest is slow compared with the time to collect a single interferogram. Then multiple interferograms can be collected, each corresponding (roughly) to a different time delay after initiation of the transient. This method is limited to time constants greater than ~10 ms, and the achievable resolution drops as scan time is reduced.

The next easiest variant of continuous-scan TRFTS occurs when the time constant of the signal is short compared with the time between the fringes of the interferogram of a He–Ne laser, which shares part of the interferometer optics. The transients are usually triggered at the occurrence of a signel created in some fixed relation to the He–Ne fringes. The sampling happens a preset delay time later when the mirror may be positioned between He–Ne fringes. If the mirror speed is stable or the delay time is very short, then the spatial offset can be considered as constant. Then the mandatory phase correction removes any asymmetry this offset introduces in the interferogram. The minimum digitizing rate is limited by the speed of the moving mirror to greater than several hundred hertz in practice, so this method is confined to transient events that are shorter than ~100 μs and that can be repeatedly excited at rates of ~1 kHz. The latter requirement is especially hard to realize if the excitation source needs to be a high-energy pulsed laser.

The solution, and most difficult continuous-scan method of TRFTS, is the stroboscopic or interleaved method.[1] Here, interferogram points are skipped both to allow use of low duty-cycle excitation sources and to permit study of transients longer than the digitizing period. Missing points are collected dur-

The authors are with the Department of Physics, University of Central Florida, Orlando, Florida 32816.

Received 29 June 1995; revised manuscript received 12 October 1995.

0003-6935/96/162849-08$10.00/0

ing subsequent sweeps and sorted later into complete interferograms. (The method of intermediate difficulty above is clearly a limiting case of the stroboscopic method.) The problem of luminenscence and energy transfer in rare-earth activated laser crystals, which initiated our work, requires the stroboscopic method if a continuously scanning instrument is to be used.

The step-scan method is progressing more rapidly than continuous-scan methods.[2–4] However, there is reason to continue development of TRFTS with continuously scanning instruments. These machines have the advantage of a relatively simple drive mechanism and the possibility of using dynamic alignment. The number of continuously scanning instruments in the field is enormously larger than the number of commercial step-scan instruments. The availability of a low-cost add-on that uses only the He–Ne reference and white-light-interferogram zero-path-length-difference (ZPD) indicator common to all commercial Fourier-transform infrared (FTIR) spectrometers, together with the signal of interest, would make TRFTS available to thousands of present users. Such an add-on should introduce no (or trivial) hardware changes to the mirror drive, and it must automatically recognize and correct sources of artifacts.

Artifacts in TRFTS stem from the requirement that thousands of transient events be repeated to complete an interferogram. A typical event is luminescence excited by a pulsed laser. Each transient signal should have the same amplitude and time dependence, but these requirements are violated if the excitation source has shot-to-shot intensity fluctuations or missed shots. All data in an interferogram at some desired time delay should actually be collected at that delay. However, for measuring at known path-length differences, sampling is typically done at He–Ne fringes or their multiples. Timing errors from inevitable mirror speed fluctuations will cause signal fluctuations unrelated to the desired modulation by the interferometer and will therefore introduce noise or artifacts.

A separate issue is the white-light interferogram used to identify the ZPD and therefore the absolute mirror position. Most commercial FTIR spectrometers use common optics for both the white light and the signal of interest so that the ZPD condition is the same for both. In the stroboscopic method, points must be skipped and filled in during subsequent scans. Hence the spectrometer must know when to sample and when to skip for each scan. It cannot know this until the white-light ZPD establishes the absolute mirror position. Thus much of the signal of interest around the ZPD cannot be collected, but this is precisely the region needed to determine absolute intensities and to calculate the phase correction. To solve this problem, McWhirter and Sievers[5] advanced the ZPD signal by introducing an optical retardation in the path of the white light in the moving arm of the interferometer. This simple modification is required for converting most commercial continuously scanning FTIR spectrometers for TRFTS.

2. Experiment

The first step in preparing our Bomem DA-8 for TRFTS was to implement the white-light ZPD advance. Because we have done this differently from McWhirter and Sievers,[5] in a way that facilitates the high-frequency spectroscopy of interest for laser crystals, we describe our method in detail. The white light, He–Ne beam, and signal-of-interest beams all occupy different portions of common optics. Using the essentially identical Bomem DA-3, McWhirter and Sievers[5] placed a thin glass flat in the white-light path, but also in the He–Ne laser path, for the moving interferometer arm, as shown in Fig. 1A. This method has been used successfully in the mid IR.[5,6] However, because the He–Ne laser is used in many instruments, including the Bomem DA series, for dynamic alignment, this arrangement potentially reduces the modulation efficiency, especially at higher optical frequencies, because of deviations from parallelness in the optical flat. For example, a high-quality flat that is parallel to 1 arc sec introduces a slight difference in path length between different parts of the He–Ne beam. The dynamic alignment system senses and tries to eliminate this difference, but in the process introduces a mirror tilt amounting to a path-length difference of 0.5 μm over the full 10-cm mirror diameter. This tilt is equivalent to one full wavelength in the green. Hence any alteration of the path of the alignment laser should be avoided. Our solution is to place the optical flat only in the path of the white light. Figure 1B shows this setup. The cross section of the laser light is L shaped and somewhat encloses the

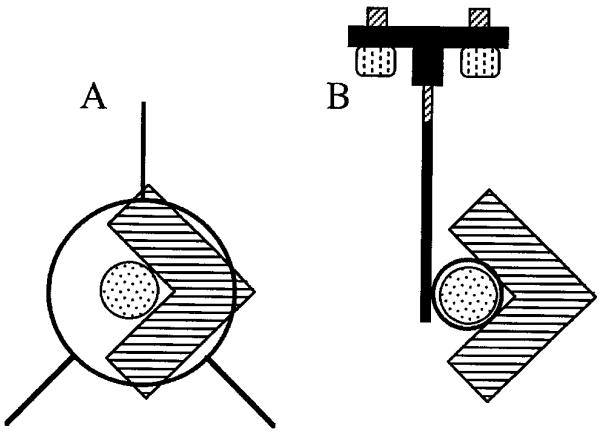

Fig. 1. White-light-interferogram (ZPD indicator) advancement schemes for the Bomem DA series. The L shaped object is the He–Ne alignment laser beam with fringes indicated. The shaded circle is the white-light beam. The open circle represents the optical flat. Method A is that devised by McWhirter and Sievers,[5] in which the flat hangs from above and intercepts both white-light and He–Ne beams. Method B is our method, in which the flat is mounted to the back wall with push–pull screws. Method B leaves the He–Ne alignment laser beam unaffected.

white-light beam. The holder of the uncoated quartz flat (10 mm × 0.5 mm, parallel to <0.5 arc sec) is adjusted by the use of push–pull screws such that the flat fully covers the white light but leaves the alignment beam unaffected. Optical flats of diameter equal to that of the white-light beam, sufficiently parallel to allow a reliable detection of the white light (mostly from near IR) and as thick as necessary for the intended advancement of the ZPD signal, are readily available. Our flat was obtained from Lightning Optics. Another advantage is that this setup avoids scattering from this additional optical element of He–Ne laser light into the signal detector (a known source of artifacts).

With the addition of the white-light ZPD advancement, reasonably good results can be obtained with stroboscopic TRFTS software from Bomem. Representative spectra appear in Refs. 5 and 6. We have used this software to collect time-resolved spectra of the photoluminescence of 2% Nd in 300 K $Sr_5(VO_4)_3F$ at 6 cm^{-1} resolution by using long-pulse excitation from a laser diode. A spectrum taken 63 μs after the excitation is terminated is compared with a cw spectrum in Fig. 2. The major difference is the disappearance of the excitation light in the time-resolved spectrum. However, a closer look (inset) reveals an artifact: a periodic derivativelike structure of small amplitude is superimposed on the time-resolved spectrum. Even though this experiment was designed to exert only modest demands on the TRFTS system, artifacts appear that the commercial implementation is unable to avoid or to recognize and correct automatically. In actual laser-crystal experiments of interest, the frequency and the time resolutions will be higher, and a more powerful, but much less stable, short-pulse laser will be used. The commercial TRFTS implementation is therefore essentially useless for laser-crystal spectroscopy.

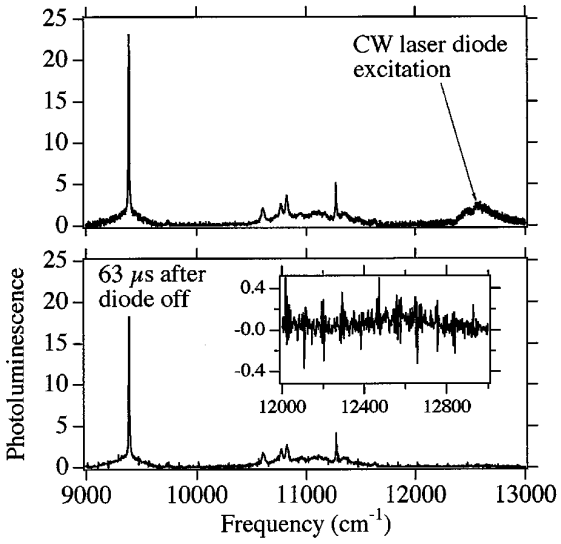

Fig. 2. Low-resolution (6-cm^{-1}) luminescence spectra of 2% Nd^{3+} in 300 K $Sr_5(VO_4)_3F$. The two groups of sharp lines below 12,000 cm^{-1} are the $^4F_{3/2} \rightarrow {}^4I_{9/2,11/2}$ bands. The upper spectrum is obtained from a single-scan interferogram in the usual cw mode, and the partially filtered laser diode excitation is observed near 12,800 cm^{-1}. The lower spectrum was obtained from a single complete interferogram collected with the commercial TRFTS package (Bomem). Emission from the diode has almost completely disappeared while the crystal continues to emit. The inset shows the presence of periodic artifacts in the TRFTS spectrum.

We next discuss the known sources of artifacts and the solutions we have adopted in our first, home-built stroboscopic TRFTS implementation. The first of these are variations in excitation intensity, which cause variations in the amplitude of the transient signal. Random variations will contribute noise, and systematic variations will cause artifacts that can easily be mistaken for real spectral features,[1] as in the inset of Fig. 2. They can also cause variations in the spectral content or in the time dependence of the transient if secondary processes with a nonlinear dependence on excitation intensity contribute to the signal.

Several practitioners of both continuous- and step-scan methods have noted the significant signal-to-noise advantages to be gained by correcting for laser shot-to-shot variations.[7,8] The method of Lindner *et al.*[7] consists of dividing the transient signal measured at the desired delay time by the time integral of the luminescence intensity measured with a second detector. The division is done by an analog circuit before the data are digitized by the analog-to-digital converter (ADC). The method of Heard *et al.*[8] measures the laser energy and uses it for the correction by software.

Our method differs in the following respects. We avoid specialized electronic equipment (such as precision gate, integrator, and divider) and capitalize on our ADC's (Keithley DAS1800-HR2) ability to sample different channels in a preprogrammed order. A schematic of our setup is shown in Fig. 3. Before each transient is excited, the ADC samples both the

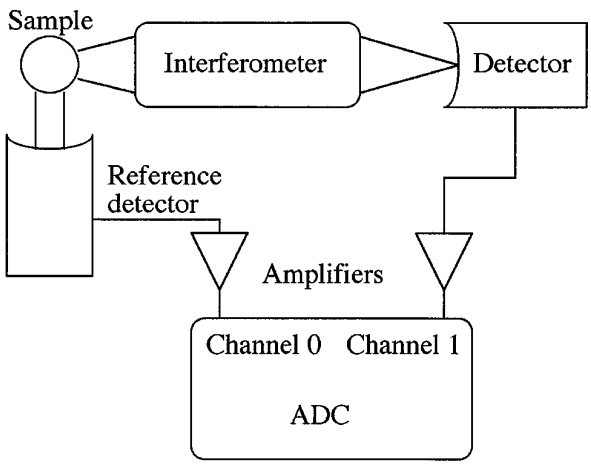

Fig. 3. Schematic of our TRFTS method for correcting intensity fluctuations. The reference signal is taken directly from sample luminescence. Both signal and reference channels are separately digitized by the ADC.

interferogram and the reference channels to determine the current zero levels. After the excitation of each transient, the interferogram channel is digitized at the times of special interest. In the unused time slots (mostly for longer times) with sufficient signal, the reference channel is sampled. As long as the reference samples are taken at the same delay times for each transient, they can be zero corrected and added to give a quantity I_0, which is proportional to the transient's intensity (numerical integration). The numerical division of interferogram samples from the same transient by I_0 removes the variable intensity information. Multiplying the entire interferogram with the average of I_0 over all transients returns the average intensity information. This latter feature of our normalization method allows the quantitative comparison of spectra from different specimens and is an advantage over methods that use analog division.[7] Using the sample itself as the source for the reference senses the energy actually absorbed and avoids problems like the pointing instabilities of the pump laser and multiphoton absorption.

Our correction method scales the signal linearly. Because the reference is derived from the sample (rather than from the excitation source[8]), the method works also if there are nonlinear processes that affect only the sample's initial conditions. If there are nonlinear processes that change the temporal shape or the spectral content of the transients, one has to restrict the use of such a method to a small range of excitation intensities. Therefore we have also implemented a method for recognizing when the laser provides an intensity below or above some arbitrary threshold. For that, a simplified version of I_0 calculated in real time is used to decide the acceptance of each shot. Sweeps in which bad shots occur are then automatically repeated. This feature is extremely useful with some gas lasers in which the spark discharge is random in nature, such as N_2 lasers.

A more insidious problem is timing jitter, to correct which title effort has been expended to date. Timing jitter can arise from mirror-speed fluctuations caused by surface roughness, discreteness of moving electrical contacts, imperfections in the speed sensing and control system, external disturbances, etc. Figure 4 shows, for a hypothetical data acquisition with three skipped points, how mirror-speed variations translate into timing jitter. The delay times of the digitizing events are plotted versus their fringe number. To obtain the spectral information at fixed intervals, sampling is done in fixed relation to the He–Ne fringes, i.e., full and half fringes in Fig. 4. Each He–Ne fringe corresponds to 633 nm of path-length difference. The time t the mirror needs to travel between sampling locations sets the spacing of the samples in the time domain. However, because the mirror speed can vary, the sampling times are uncertain, which is indicated by the error bars. This is especially critical if one uses, to accommodate slow transients, slow speeds in which the speed-sensing signal is weak (noise) and the slopes in Fig. 4 are steep. Figure 5 presents speed data for an optimized vertically scanning Bomem DA-8 at 0.07 cm/s. In this figure, the times between He–Ne laser fringes are plotted versus path-length difference. Both noise of varying amplitude and a slow drift are evident.

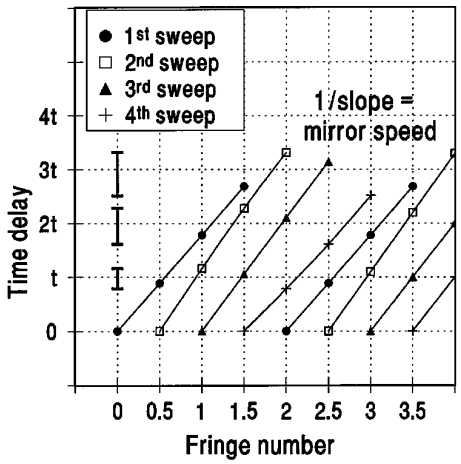

Fig. 4. Schematic of continuous-scan stroboscopic data acquisition of visible time-resolved spectra. Samples (indicated by symbols) are taken at certain fractions (shown is 1/2) of He–Ne fringes. The delay time t is controlled by the time the mirror needs to travel to the next sampling location. The arising timing jitter is represented by the error bars.

Our TRFTS method treats the different types of mirror-speed fluctuation in a number of ways. First we optimize the adjustment of the feedback of the commercial speed control. There still remains the possibility of large and rapid fluctuations, which can desynchronize the mirror motion with the interferogram sampling, because several (4 or 8) samples per He–Ne fringe are needed at visible–UV frequencies. For the case of four samples, the Bomem DA-8 inserts three ADC triggers between He–Ne fringes.

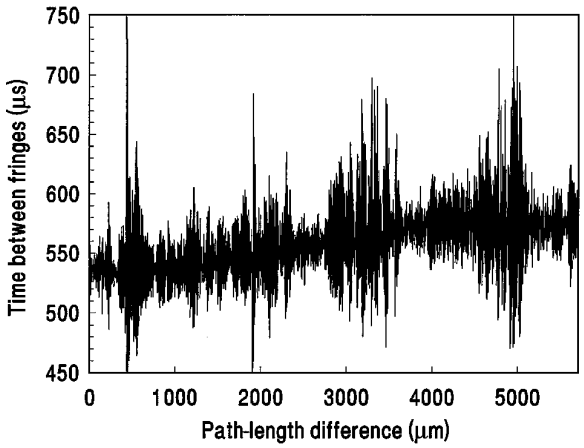

Fig. 5. Time between He–Ne fringes at one of the slowest available mirror speeds versus path-length difference. The nominal speed is 0.07 cm/s. The drive mechanism is unmodified. Mirror-speed noise of varying amplitude and a drift are evident.

These extra triggers are spaced in time by 25% of the measured previous fringe-pair period. If the mirror undergoes a brief and rapid acceleration, such that the next He–Ne fringe signal arrives before the third extra trigger, one ADC sample is lost. Without a provision to recognize such errors, all samples to the end of that sweep are associated with the wrong path-length difference. Our electronics recognizes such mistakes and repeats the entire sweep.

The smaller, but much more frequent, speed variations are also a problem. Figure 6 presents the variations about an intended speed of 0.5 cm/s as determined from the time between He–Ne fringes (1-μs resolution) for a small part of the total sweep. The upper trace was taken with unmodified Bomen DA8 drive hardware after careful adjustment of the speed control feedback. Frequent deviations of approximately ±2% are evident in this trace. To reduce these variations, we further stabilized the mirror speed by counterbalancing the vertically moving mirror with an external pulley and weight. This reduces the torque required of the driving motor. The stabilizing effect is evident in the lower trace of Fig. 6, in which only few deviations exceed the digitizing noise.

To study the effect on the spectra of our simple mechanical correction for mirror-speed fluctuations, we built the LED circuit in Fig. 7, which gives a near-IR off–on transient with a 200-μs transition time. Figure 8 shows the resulting spectra without the counterweight. Figure 9 shows the spectra taken while the counterweight was used. A resolution of 5 cm^{-1} was chosen for all spectra to obtain clearly visible noise, which is less in Fig. 9. At t = 252 μs, the signal-to-noise ratio at the peak is ~2 without the counterweight; this is improved by using the weight to a value of ~5. In addition, observe that the noise is worse during the early and most rapidly changing part of the transient. This confirms that noise originates in timing jitter, as this is

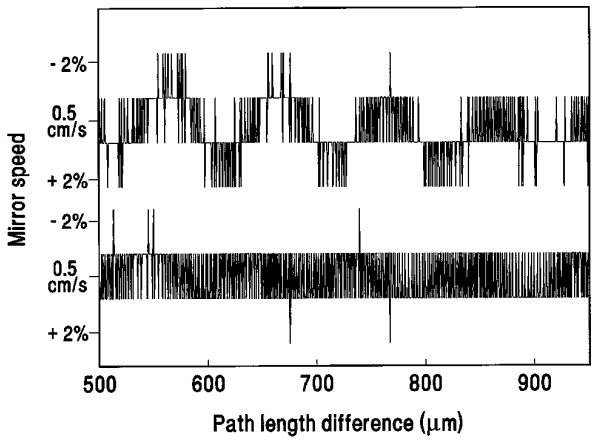

Fig. 6. Comparison of the mirror-speed stability with (lower trace) and without (upper trace) a counterweight's balancing the vertically moving mirror at a nominal speed of 0.5 cm/s. The digital noise steps for the time between He–Ne fringes have a value of 1 μs.

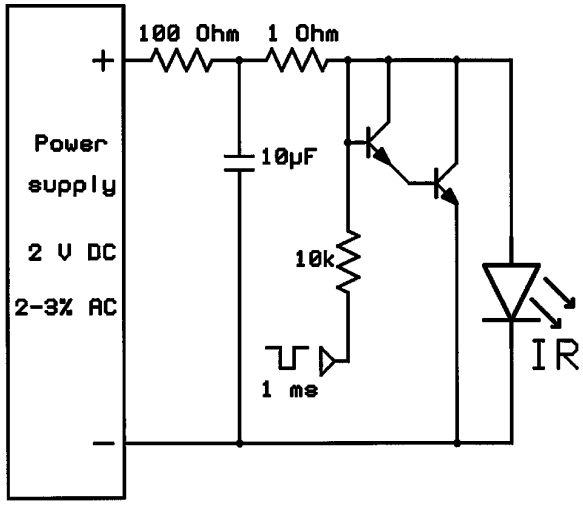

Fig. 7. Electrical circuit used for testing our TRFTS system. A negative going pulse at the input allows the LED to turn on. The 2%–3% ac ripple on top of the dc supply simulates actual shot-to-shot variations expected from a good pulsed laser source.

precisely where timing jitter would cause the largest uncertainty in the measured intensity.

The slow drifts evident in Fig. 5 are not currently corrected and are possibly the reason for some of the remaining noise or artifacts in Fig. 9.

Figures 6, 8, and 9 show that timing-jitter noise is reduced but not eliminated by the counterweight. The remaining timing noise is unavoidable because the interferogram needs to be sampled in identical intervals (the He–Ne fringes or even fractions). Because 2% timing jitter translates into approximately 2% signal noise, the noise becomes larger

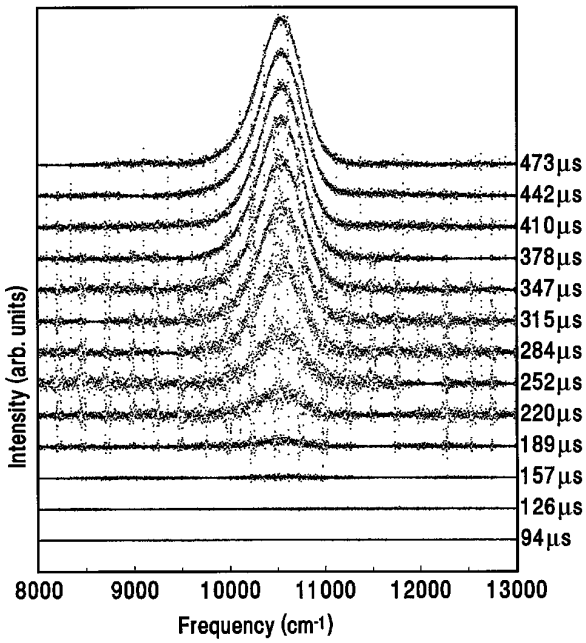

Fig. 8. Time-resolved spectra of a LED during turn-on as taken with our TRFTS data-acquisition system at a mirror speed of 0.5 cm/s and an unmodified interferometer drive. The resolution was 5 cm^{-1}.

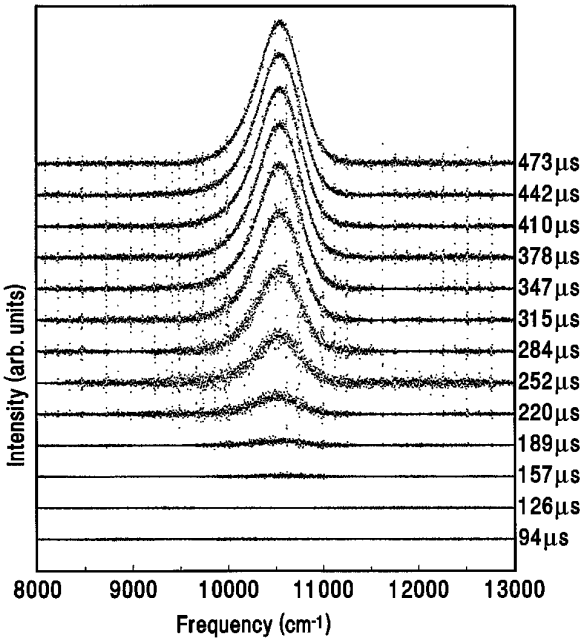

Fig. 9. Time-resolved spectra of a LED during turn-on as taken with our TRFTS data-acquisition system at a mirror speed of 0.5 cm/s in which the timing jitter has been reduced by the counterbalancing of the mirror weight. The resolution was 5 cm^{-1}.

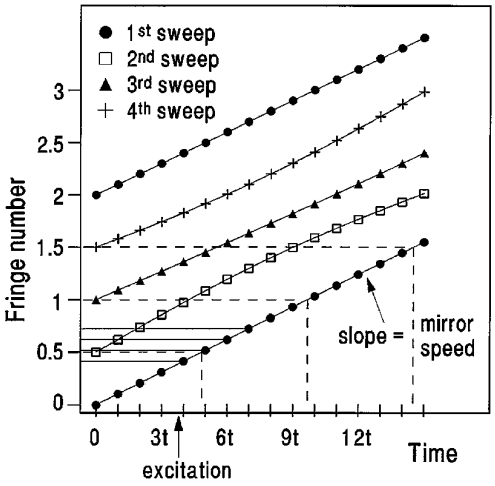

Fig. 10. Schematic of a proposed continuous-scan stroboscopic data-collection method that eliminates timing jitter caused by mirror-speed variations. Interferogram sampling within each sweep starts (in this case) at integer multiples of half He–Ne fringes and continues in constant time intervals t until the interesting part of the transient is over. This pattern is repeated with offset steps of half fringes to fill the remaining gap. The mirror speed is measured by the collection of the arrival times of the fringe signals (dashed lines), and this speed is used to determine the fractional fringe numbers for each sample (horizontal solid lines).

than the interferometer modulation at a long path-length difference. Therefore the quality of the spectra is expected to degrade as resolution increases. Hence timing jitter may render this implementation of TRS unsuitable for some laser-crystal studies.

We propose the following next-generation TRS implementation that should drastically reduce the remaining timing-jitter noise. The interferogram, in fact, needs to be only known at points with equal path-length-difference spacing, not necessarily measured at these points. Figure 10 illustrates the principle of the new data-collection scheme. Mirror position versus time is plotted for a hypothetical collection case, in which four sweeps are required for completing a single interferogram that has two samples per fringe. Each sampling cycle starts when the mirror reaches some preset path-length difference (for the first sweep: 0, 2, 4, . . .). The samples (represented by the symbols) are no longer directly synchronized to the motion of the mirror. Sampling is done at a stabilized rate suitable for the ADC used. The timing jitter is then reduced to the time-base uncertainties, the time jitter of the excitation source, and that of the ADC itself. Therefore the time resolution and the timing accuracy now have the same limitations as for step-scan interferometers. The advantage of greatly reduced timing jitter comes at the expense of losing the exact information about the sample's position in the interferogram. The mirror-speed variations translate now into variations of the He–Ne fringe positions with respect to the frame set by the ADC samples (dashed lines in Fig. 10). However, by measuring the times at which the He–Ne fringes occur and interpolating with a polynomial, one can find the mirror speed as a function of time and the path-length difference (horizontal solid lines) at which each ADC sample occurred. (This method is similar to one mentioned by Brault.[9] He reports no observable degradation from slow variations in velocity of a few percent.) The result is now a list of interferogram intensities plus a list of corresponding path-length differences (one pair of lists for each time delay sampled by the ACD). The average spacing between list entries is determined by the effective spacing of the excitation events, which is set by the starting positions of the sampling cycles. It is important that the average spacing between the measured data points can be chosen to be as small as necessary. Small deviations from the average spacing, which arise from mirror-speed noise, do not cause any loss of information if the interferogram was sufficiently oversampled, i.e., as long as the largest gap between samples still corresponds to an optical frequency high enough to avoid aliasing. Hence we have established a method of collecting the complete information of time-dependent interferograms. The method is somewhat related to the asynchronous TRFTS reported by Masutani *et al.*[10] The most significant difference is our stroboscopic acquisition of the data, which makes impossible the electronic filtering of unwanted information. However, there is no principal reason why this could not be done numerically. Thus the problem has been reduced to the need of a suitable interpolating digital filter.

Brault[9] has successfully implemented such a filter, which finds interferogram values at unevenly spaced points from a list of evenly spaced samples. Our problem is numerically more demanding because the available list of data is not equally spaced. However, the principal function is the same. For small speed variations, the interpolation is always done very close to a measured point. Therefore even simple (fast and reliable) interpolation schemes should work well.

A different approach could be least-squares fitting of harmonic functions to the interferogram. The procedures given in Ref. 11 seem to provide a good starting point. Implementation of these ideas is in progress, and preliminary results are promising.

3. Application to Laser Crystals

To illustrate the potential of our TRFTS implementation, we describe one specific application, namely, dynamic energy-transfer processes that occur in rare-earth activated insulators for laser and phosphor applications. These materials have sharp spectral features and important dynamic effects whose spectral signatures span the IR, visible, and UV. Johnson *et al.*[12] have measured the time-dependent emission of a *Q*-switched YLF laser by using TRFTS, although theirs was not really a spectroscopic study, merely a measure of the time dependence of the diode laser excitation and the subsequent *Q*-switch pulse.

Laser crystals, because of their complexity, can potentially be studied more effectively by TRFTS than by other existing techniques. After an excitation, a large variety of local or collective processes (up and down conversions) redistribute the energy in the ensemble of different ions, each with numerous levels throughout the IR, visible, and UV. The time evolution of the various level populations can be investigated by the observation of the time-resolved photoluminescence originating from (most) of these levels. Transfer and decay rates can then be determined and used to optimize dopant concentrations. In addition, because many more compounds are known in powder form than have been grown as single crystals, measurements on powders can be used to identify in advance those worth further effort at crystal growth.

Rare-earth photoluminescence lines are often less than 0.25 cm^{-1} wide at low temperatures and range from the IR to the UV. These range and resolution requirements are readily met by TRFTS with the Bomen DA-8. Because lifetimes of rare-earth ions in insulating crystals often fall in a range from 100 μs to 10 ms, stroboscopic data acquisition will frequently be the method of choice. Our relatively slow Nd:YAG laser (Spectra Physics GCR150-30 Hz) can be used. Its doubled or tripled output pumps a tunable dye laser (Laser Photonics DL-14), whose narrow linewidth (0.3 cm^{-1} at 580 nm) allows excitation to single energy levels of single species and selection of single crystallographic sites in multisite crystals. In fact, an up-conversion laser crystal with six different doping sites will be our first application. TRFTS will provide information on the transfer dynamics, which will find use in optimizing dopant concentrations and growth conditions.

4. Summary

A home-built add-on for a continuously scanning Fourier spectrometer to allow time-dependent measurements was reported. Features include (1) a new way of ZPD indicator advancement, which permits dynamic alignment to work as intended without loss of high-frequency modulation efficiency; (2) a method to normalize excitation intensity fluctuations with several advantages over previous schemes; (3) automatic recognition of missed excitations and scan repeat; (4) a simple mechanical modification of the drive mechanism to reduce mirror-speed variations; and (5) automatic recognition of major errors caused by timing jitter from mirror-speed variations. The effects on interferograms and spectra of timing jitter were discussed, and a next-generation implementation of TRFTS that will reduce timing-jitter effects to a level characteristic of step-scan implementations was proposed.

This work was supported by the U.S. Air Force Office of Scientific Research (FH9620-95-1-0075) and by the University of Central Florida Division of Research and Training.

References

1. J. J. Sloan and E. J. Kruus, "Time-resolved Fourier transform spectroscopy," in *Time Resolved Spectroscopy,* R. J. H. Clark and R. E. Hester, eds. (Wiley, New York, 1989), pp. 219–253.
2. W. Uhmann, A. Becker, C. Taran, and F. Siebert, "Time-resolved FT-IR absorption spectroscopy using a step-scan interferometer," Appl. Spectrosc. **45,** 390–397 (1991).
3. R. A. Palmer, J. L. Chao, R. M. Dittmar, V. G. Gregorious, and S. E. Plunkett, "Investigation of time-dependent phenomena by use of step-scan FT-IR," Appl. Spectrosc. **47,** 1297–1310 (1993), and other papers in this issue.
4. G. Durry and G. Guelachvili, "High-information time-resolved step-scan Fourier interferometer," Appl. Opt. **34,** 1971–1981 (1995).
5. J. T. McWhirter and A. J. Sievers, "Time-resolved spectroscopy with Fourier transform spectrometers: maintaining the Fellgett advantage," Appl. Spectrosc. **45,** 1391–1394 (1991).
6. S. A. Rogers and S. R. Leone, "Pulsed laser photolysis time-resolved FT-IR emission studies of molecular dynamics," Appl. Spectrosc. **47,** 1430–1437 (1993).
7. J. Lindner, J. K. Lundberg, R. M. Williams, and S. R. Leone, "Pulse-to-pulse normalization of time-resolved Fourier transform emission experiments in the near infrared," Rev. Sci. Instrum. **66,** 2812–2817 (1995).
8. D. E. Heard, R. A. Brownsword, D. G. Weston, and G. Hancock, "Time-resolved pulsed FT-IR emission studies of photochemical reactions," Appl. Spectrosc. **47,** 1438–1445 (1993).
9. J. W. Brault, "A new approach to high-resolution FTS design,"

in *Fourier Transform Spectroscopy: New Methods and Applications,* Vol. 4 of 1995 OSA Technical Digest Series (Optical Society of America, Washington, D.C., 1995), pp. 11–13.
10. K. Masutani, H. Sugisawa, A. Yokota, Y. Furukawa, and M. Tasumi, "Asynchronous time-resolved Fourier transform infrared spectroscopy," Appl. Spectrosc. **46,** 560–567 (1992).
11. W. H. Press, S. A. Teukolsky, W. T. Vetterling, and B. P. Flannery, *Numerical Recipes in C: The Art of Scientific Computing,* 2nd ed. (Cambridge U. Press, New York, 1992), pp. 575–584.
12. T. J. Johnson, A. Simon, J. M. Weil, and G. W. Harris, "Application of time-resolved step-scan and rapid-scan FT-IR spectroscopy: dynamics from 10 seconds to 10 nanoseconds," Appl. Spectrosc. **47,** 1376–1381 (1993).